Mechanisms of cellular retention of melanin bound drugs : Experiments and computational modeling

Bahrpeyma, Sina

2022-08

Bahrpeyma , S , Reinisalo , M , Hellinen , L , Auriola , S , Amo , E M D & Urtti , A 2022 , ' Mechanisms of cellular retention of melanin bound drugs : Experiments and computational modeling ' , Journal of Controlled Release , vol. 348 , pp. 760-770 . https://doi.org/10.1016/j.jconrel.2022.05.059

http://hdl.handle.net/10138/347739
https://doi.org/10.1016/j.jconrel.2022.05.059

Journal of Controlled Release 348 (2022) 760–770

Contents lists available at ScienceDirect

Journal of Controlled Release

journal homepage: www.elsevier.com/locate/jconrel

Mechanisms of cellular retention of melanin bound drugs: Experiments and computational modeling

Sina Bahrpeyma [a,b,*], Mika Reinisalo [a], Laura Hellinen [a], Seppo Auriola [a], Eva M. del Amo [a], Arto Urtti [a,b,c,*]

[a] School of Pharmacy, Faculty of Health Sciences, University of Eastern Finland, 70210 Kuopio, Finland
[b] Faculty of Pharmacy, University of Helsinki, 00014, University of Helsinki, Finland
[c] Institute of Chemistry, St. Petersburg State University, Petergoff, Russian Federation

ARTICLE INFO

Keywords:
Pigment
Melanin binding
Melanosome
Retinal pigment epithelium
Ocular pharmacokinetics
Modeling

ABSTRACT

Melanin binding of drugs is known to increase drug concentrations and retention in pigmented eye tissues. Even though the correlation between melanin binding *in vitro* and exposure to pigmented eye *in vivo* has been shown, there is a discrepancy between rapid drug release from melanin particles *in vitro* and the long *in vivo* retention in the pigmented tissues. We investigated mechanisms and kinetics of pigment-related drug retention experimentally using isolated melanin particles from porcine retinal pigment epithelium and choroid, isolated porcine eye melanosomes, and re-pigmented ARPE-19 cells in a dynamic flow system. The experimental studies were supplemented with kinetic simulations. Affinity and capacity of levofloxacin, terazosin, papaverine, and timolol binding to melanin revealed K_d values of ≈ 50–150 μM and B_{max} ≈ 40–112 nmol.mg^{-1}. The drugs were released from melanin in <1 h (timolol) or in 6–12 h (other drugs). The drugs were released slower from the melanosomes than from melanin; the experimental differences ranged from 1.2-fold (papaverine) to 7.4-fold (timolol). Kinetic simulations supported the role of the melanosomal membrane in slowing down the release of melanin binders. In release studies from the pigmented ARPE-19 cells, drugs were released from the cellular melanin to the extracellular space in ≈ 1 day (timolol) and ≈ 11 days (levofloxacin), *i.e.*, much slower than the release from melanin or melanosomes. Simulations of drug release from pigmented cells in the flow system matched the experimental data and enabled further sensitivity analyses. The simulations demonstrated a significant prolongation of drug retention in the cells as a function of decreasing drug permeability in the melanosomal membranes and increasing melanin content in the cells. Overall, we report the impact of cellular factors in prolonging drug retention and release from melanin-containing cells. These data and simulations will facilitate the design of melanin binding drugs with prolonged ocular actions.

1. Introduction

Pharmacological treatment of the ocular anterior segment (*e.g.* inflammations, elevated intraocular pressure) is practiced with small molecule drugs that are given topically in eye drops at intervals of 1–8 eye drops daily, depending on the indication and drug [1]. Frequent application rates and difficulties in the eye drop instillation lead to reduced patient compliance; for example, about 50% of glaucoma patients do not use their medications properly [2]. Some pharmaceutical approaches have been used to prolong the instillation intervals (*e.g.* microparticles, inserts, gels) [3,4], but no technology has reached wide use in the clinics.

The posterior eye segment is treated mostly with drugs that are given as intravitreal injections [5]. This applies to some biologicals (*e.g.* anti-

Abbreviations: app k_{off}, apparent dissociation rate constant; ARPE19-mel, artificially re-pigmented ARPE-19 cells; B_{max}, maximum binding capacity; $C_{cytosol}$, free drug concentration inside cytosol; C_{mel}, free drug concentration inside melanosome; K_d, equilibrium dissociation constant; k_{off}, dissociation rate constant; k_{on}, association rate constant; L, free ligand concentration; LC-MS/MS, liquid chromatography–mass spectrometry/ mass spectrometry; LLOQ, the lowest limit of quantification; LM, occupied binding sites; M, available binding sites; M_{tot}, total concentration of binding sites; n, heterogeneity index; NSB, nonspecific binding; $P_{app,\ apical\ or\ basolateral}$, permeability of single membrane (apical or basolateral); $P_{app,\ total}$, apparent permeability of a cell monolayer; RPE, retinal pigment epithelium; SA, surface area; UPLC, ultra-performance liquid chromatography.

* Corresponding authors.
E-mail addresses: sina.bahrpeyma@uef.fi (S. Bahrpeyma), arto.urtti@uef.fi (A. Urtti).

https://doi.org/10.1016/j.jconrel.2022.05.059
Received 18 February 2022; Received in revised form 22 April 2022; Accepted 15 May 2022
Available online 25 June 2022

VEGF antibodies, soluble receptors), but small molecules are eliminated from the vitreous in a few hours making clinical treatment with injectable solutions impractical [6,7]. In the case of corticosteroids, poorly soluble suspensions (*e.g.* triamcinolone acetonide) or controlled release implants (*e.g.* dexamethasone releasing Ozurdex) have been used to extend the duration of drug actions [8]. However, a short duration of action remains a major hurdle in the development of small molecule drug treatments for retinal diseases.

Successful prolongation of pharmacological effects would benefit ophthalmic drug discovery and development. Melanin binding of drugs in the eye is an interesting phenomenon that has implications in the prolongation of drug actions. Melanin is an insoluble endogenous polymer that is located in the melanosomes of pigmented cells in the iris, ciliary body, retinal pigment epithelium (RPE), and choroid [9]. It is known that many drugs (*e.g.* brimonidine, betaxolol, levofloxacin, atropine, timolol) bind to melanin, leading to elevated drug concentrations and prolonged retention in the pigmented eye tissues [10–13]. Half-life of declining mydriatic response after topical atropine instillation was 43 h in albino rabbits, whereas extended half-life of 96 h was seen in pigmented rabbits [14], which is in line with the slow recovery of human eyes (1–2 weeks) from atropine effects. Likewise, the miotic response *vs* time curve after instillation of topical 4% pilocarpine solution showed 1.8 times slower response decay in pigmented rabbits than in the albino rabbits [15]. This resulted in 3.3 times higher area under the miotic response *vs* time curve in pigmented animals as compared to the albino rabbits. More recently anti-VEGF agent pazopanib and its analogue GW771806 showed depot effect in pigmented rats after per oral dosing [16]. Pigment binding and retention of 35 days were demonstrated as well as anti-neovascular effects in pigmented mouse and rat models.

Even though the melanin binding of drugs has been known for decades, the chemical drivers of melanin binding have been investigated and revealed only recently [17,18]. This paves way for drug discovery approaches that utilize melanin binding as the pharmacokinetic key factor. Correlation of *in vitro* melanin binding and *in vivo* retention in the tissues was shown recently, but the striking difference (orders of magnitude) was seen between short drug retention in melanin particles *in vitro* and long retention in the pigmented rat eyes *in vivo* [19]. Based on theoretical simulations we suggested that interplay between melanin binding and cell membrane permeability may extend drug retention in the pigmented cells [20]. In this study, we performed a systematic and mechanistic study to investigate drug retention in melanin, melanosomes, and pigmented cells to understand the interplay of various factors in sustained drug release from pigmented cells. The experiments were supported with kinetic simulations.

2. Materials and methods

2.1. Materials

Levofloxacin, terazosin hydrochloride, papaverine hydrochloride, timolol maleate, and all other reagents were purchased from Sigma-Aldrich, Germany. Stock solutions of 50 mM in DMSO were prepared for levofloxacin, and timolol whereas 12.5 mM and 10 mM solutions were used for terazosin and papaverine, respectively. Further dilutions were made in either Hank's balanced salt solution (HBSS pH 7.4, with $CaCl_2$, $MgCl_2$) or Dulbecco's phosphate-buffered saline (DPBS pH 7.4, without $CaCl_2$, $MgCl_2$) from Gibco (Thermo Fisher Scientific, Waltham, MA, USA). Dulbecco's Modified Eagle Medium/Nutrient Mixture F-12 (DMEM/F-12, Gibco, Cat No. 31330–038) supplemented with 10% FBS (Fetal bovine serum), and 1% penicillin/streptomycin were used to culture ARPE-19 cells (ATCC, Manassas, VA, USA). Acetonitrile was purchased from Honeywell (Seelze, Germany) and formic acid from Merck (Darmstadt, Germany). Internal standards for mass spectrometry (levofloxacin D8, terazosin D8, papaverine D3, rac timolol-d5 maleate) were purchased from Toronto Research Chemicals (Toronto, ON, Canada).

2.2. Studies with melanin and melanosomes

Melanin was isolated from the RPE and choroid of the porcine eyes as described elsewhere [21], and the melanin was stored at −20 °C until use. Intact RPE melanosomes were isolated from fresh porcine eyes as previously described elsewhere [22]. Drug release from melanin and melanosomes was investigated based on the previous method for melanin [19] with slight modification. The isolated melanin was weighted and sonicated for 15 min at 37 °C in a bath sonicator (Elmasonic S 40H, Elma Schmidbauer GmbH, Singen, Germany) to form a homogenous suspension prior to the experiment. Melanin suspension (0.1 $mg.mL^{-1}$) was prepared in HBSS buffer with 5 mM ATP at pH 7.4. Similarly, isolated melanosomes (0.1 mg mL^{-1}) were suspended into HBSS buffer containing ATP (5 mM, at pH 7.4). Next, the melanin and melanosome suspensions were exposed to a concentration of 100 μM (levofloxacin, timolol, terazosin, or papaverine) in a total volume of 100 μL for 2–5 h at 37 °C on a shaker (at 250 rpm). Following the drug exposure, the drug-loaded melanin and melanosomes were centrifuged at 2800*g* for 10 min at room temperature and the pellets were resuspended in a 10 mL of HBSS buffer with 5 mM ATP.

Samples of 100 μL were collected at defined time points during 24 or 48 h (terazosin and timolol in melanosomes samples only). All the samples were centrifuged immediately at 14000*g* for 1 min and 60 μL of supernatant was mixed with 60 μL of acetonitrile that contained 0.2% formic acid. Thereafter, these new solutions were further centrifuged at 15000*g* for 15 min and 10 μL of internal standard was added to 90 μL of the supernatant and stored at −80 °C prior to the analyses with liquid chromatography coupled with tandem mass spectrometry (LC-MS/MS). All the experiments were performed at least in triplicate.

Melanin content of isolated melanosomes was determined using spectrophotometry at absorbance of 690 nm (Varioskan LUX™ Multimode microplate reader, Thermo Fisher Scientific). Dilution series of melanin suspensions (0, 0.05, 0.1, 0.25, 0.5, 1 and 2 $mg.mL^{-1}$) was used as a reference standard for quantification of melanin in the intact melanosomes. In addition, a sample of intact melanosomes was sonicated for 15 min at 37 °C to release melanin and its melanin content was quantitated.

2.3. Studies with pigmented cells

2.3.1. Culture and re-pigmentation of ARPE-19 cells

ARPE-19 cells were cultured in supplemented DMEM/F-12 using T25 or T75 cell culture flasks at 37 °C and in the presence of 7% CO_2 [23]. The cells were sub-cultured every 7 days and the growth medium was changed every 3–4 days. Passages 11–29 were used in these studies. ARPE-19 cells do not display pigmentation in these normal growth conditions.

Twelve to fourteen days prior to the release studies, ARPE-19 cells were seeded on glass coverslips (Menzel™ Microscope Coverslips CAT#CB00120RA1, 12 mm in diameter) within 24-well plates (Nunclon Delta surface, 1.9 cm^2/well, Thermo Scientific) at a density of ~75,000 cells/well. The glass coverslips were first coated aseptically with collagen (Collagen from rat tail, Bornstein and Traub Type I, powder, BioReagent, C7661-5MG, Sigma-Aldrich) for 3 h (10 $\mu g/cm^2$), sterilized with 70% ethanol, and rinsed twice with DPBS buffer prior to cell seeding. Medium renewal (50–75% of medium) was carried out every other day for 12–14 days. Four to five days post-seeding, the coverslips became confluent with ARPE-19 cells. *Re*-pigmentation of ARPE-19 cells was performed as described earlier, with slight modifications [24]. ARPE-19 cells were exposed to different doses of isolated melanosomes (the equivalent of 23.0, 38.5, 57.5, 115, and 230 μg of melanin per well). To achieve even cellular pigmentation in the wells, the medium was mixed using pipetting during the first three days (days 5–8) and 50–75% of the medium was changed every second day. After 12–14 days post-

seeding, the ARPE19-mel (artificially re-pigmented ARPE-19) cells were used in the uptake study.

The cell viability was assessed at many stages to ensure that the cells remain functional. AlamarBlue™ cell viability protocol (alamarBlue™ Cell Viability Reagent CAT No: DAL1100, by Invitrogen) was performed before the drug uptake study, at the end of drug release study, and during method optimization. All tests were performed at least as three replicates.

2.3.2. Cellular uptake of timolol and levofloxacin

Prior to drug uptake, the cells were washed twice with HBSS buffer to remove non-internalized melanosomes and FBS from the wells. The coverslips with cells (ARPE19-mel) and two control coverslips (coated and non-coated) in 24-well plates were included in the study. The cells were exposed to 20 μM of timolol or levofloxacin in serum-free DMEM/F-12C for at least 18 h (on a shaker at 175 rpm). Three different aliquots, from ARPE19-mel, controls coverslips with and without collagen coating, were collected from each well before and after incubation with drug solutions. All the experiments were performed at 4–6 replicates.

2.3.3. Cells in dynamic flow system

The cells were investigated in dynamic flow system (Quasi Vivo®) [25,26] with 6-channel peristaltic pump (Parker Polyflex), 6 parallel chambers, and 30 mL reservoir bottles (Supplementary Fig. S1). To study drug release from pigmented cells, we optimized the conditions in the dynamic flow system. First, ARPE-19 cells were cultured on non-coated coverslips and incorporated into the flow system at different flow rates (104, 159, 190, and 250 μL.min^{-1}). The cell viability was tested and compared to the static condition. The water evaporation was determined with supplemented medium over the course of 14 days, then the media with and without FBS were evaluated, and the evaporated volume was compensated at 24 h intervals with a fresh medium.

The DMEM/F-12 medium supplemented with 10% FBS and 1% penicillin/streptomycin showed ideal viability up to 18 days when 50% of the medium was changed every 3–7 days. The flow rate of 159 μL.min^{-1} was selected for the assays (Supplementary Fig. S2.). ARPE19-mel cells remained viable in these conditions, and collagen-coated coverslips were used to optimize melanosome uptake and cell viability.

2.3.4. Drug release from the pigmented cells

Immediately after drug uptake, the ARPE19-mel cells were washed with cold HBSS buffer to remove non-associated drug and the cells on coverslips were transferred to Quasi Vivo® (with 20 mL of medium) in an incubator at 37 °C. At each time point, 100 μL of the sample was collected from reservoir bottles (or mixing chamber) and replaced with 100 μL of fresh medium. Sampling times were fixed (1, 2, 4, 6, 12, 24, 48, 96, 98, 120, 168, 170, 192, 264 and 312 h). Partial medium replacement (≈50%) was performed at 96 and 168 h. During 13 days of the release study, the evaporated volumes were replaced daily, and total medium volume was measured at the end of the experiment. Samples were stored at −20 °C before processing.

The protein in the release test samples was precipitated by adding two parts of acetonitrile with 0.1% formic acid (including the internal standard). Internal standards were levofloxacin D8, and rac timolol-d5 maleate salt. These aliquots were vortexed for 10 s followed by 10 min of centrifugation at 14000 *g* at 4 °C. Finally, 100 μL of the supernatant was collected and kept at −80 °C until liquid chromatography–mass spectrometry (LC-MS/MS) analysis.

At the end of the release experiments with pigmented cells, their melanin contents were determined using the previously described method [26]. Briefly, the cells were detached with 300 μL of TrypLE™ Express (Gibco, Thermo Fisher Scientific) and resuspended to 500 μL total volume by adding 200 μL of DPBS buffer. Then, the cell suspension was diluted with 500 μL 20% DMSO in 2 M NaOH at 70 °C for 1 h, sonicated for 15 min and absorbance was measured at 475 nm. Isolated porcine melanin was used as the melanin standard in the quantification, and it was sonicated and prepared (0, 0.05, 0.1, 0.25, 0.5, and 1 mg.mL^{-1}) similarly to the cell suspension.

2.3.5. Measurement of non-specific binding

In order to measure non-specific binding of levofloxacin and timolol in the Quasi Vivo® system, the compound solutions at concentrations of 1, 5, and 10 μM (in DMEM/F-12 medium supplemented with 10% FBS) were transferred to a dynamic flow system in a similar setting to the cellular drug release assay described above. Samples of 100 μL (with no medium replacement) were withdrawn in the beginning of the experiment and after 1, 2, 3, and 6 days to measure the variation of concentration, also medium volume at the end of the experiment was determined to measure the evaporation rate during the experiment. Finally, the protein in the samples was first precipitated by 2:1 acetonitrile to sample volume and centrifuged at 15000 *g* for 10 min, and the supernatant was further diluted 1:1 with phosphate buffer at pH 2 and the samples were stored at −20 °C to be analyzed by ultra-performance liquid chromatography (UPLC).

2.4. Analytical methods

2.4.1. LC-MS/MS analysis

Sample preparation in the release studies with melanin, melanosomes, and cells have been described above. Internal standards were levofloxacin D8, rac timolol-d5 maleate salt, terazosin D8, and papaverine D3. Calibration curves were prepared in the same manner using a background medium. In addition, six replicates of quality control samples were prepared for each compound at 1, 10, and 100 nM in order to assess matrix effects and recovery. For matrix effects, triplicates of 10 nM were prepared using 100 μL of acetonitrile with 0.1% formic acid instead of medium.

The separation was carried out using a Waters UPLC tandem mass spectrometry instrument (UPLC–MS/MS; Waters, MA, USA) on a Waters UPLC HSS T3 (1.8 μm, 2.1 × 100 mm) column at 40 °C. The injections were performed with a flow-through needle injection system using a volume range of 0.15–0.5 μL (depending on the compound). The mobile phases were 0.1% formic acid in ultrapure water (A) and 100% LC-MS grade acetonitrile (B). The gradient elution for timolol started with 90% A and 10% B (0–3 min) and continued with 100% of B (3–6 min) and the complete run time was 9 min including column wash and equilibration at a flow rate of 0.4 mL.min^{-1}. For papaverine and levofloxacin gradient with 10–95% of B at 0–3 min and a total run time of 7.5 min was used. Terazosin gradient was initiated with 10% of B at 0–0.5 min followed by 10–95% of B at 0.5–3.5 min (total run time, 6.7 min) and the flow rate was 0.3 mL.min^{-1} for these three compounds.

Mass spectrometric measurement was performed with Waters Xevo TQ-S triple quadruple mass spectrometer coupled with electrospray ionization (ESI) on a positive mode for all four compounds. Optimized MS-parameters were as follows: capillary voltage 1.5 kV (terazosin and papaverine), 3.2 kV timolol, 3.5 kV (levofloxacin); cone voltage 4 V (timolol), 80 V (terazosin), 8 V (terazosin D8), 22 V (papaverine and papaverine D3), 28 V (levofloxacin and levofloxacin D8), 2 V (rac timolol-d5 maleate); source temperature 150 °C; and desolvation temperature 500 °C (terazosin, and timolol) or 450 °C (papaverine and levofloxacin). Nitrogen (AGA, Helsinki, Finland) was used as the desolvation gas (1000 L.h^{-1} for terazosin, and timolol; 800 L.h^{-1} for papaverine and levofloxacin) and the cone gas (150 L.h^{-1}). Argon (AGA, Helsinki, Finland) was utilized as the collision gas (9 L.h^{-1}). Multiple reaction monitoring (MRM) mode was used as the scan type. The mass transitions and their respective collision energies are presented in Supplementary Table S1. The resulting data were analyzed with Waters MassLynx V4.1 software. Isopropanol injections were run between every sample to prevent any carry-over.

The lower limits of quantification (LLOQ) for the LC-MS/MS method were as follows: levofloxacin and papaverine 0.1 nM; terazosin, and timolol 0.5 nM. The lower limit of quantification (LLOQ) was considered

at a signal-to-noise ratio of 9:1.

2.4.2. UPLC analysis

The samples from non-specific binding experiments were analyzed by UPLC (Acquity UPLC, Waters, Milford, MA, USA) with UV detection (Photodiode Array Detector, Waters, MA, USA). The separation was performed utilizing a Luna Omega Polar C18 (1.6 μm, 2.1 × 50 mm) column (Phenomenex) at 30 °C. The injection volume was 5 μL and gradient mode was selected for all the compounds with an acetonitrile/15 mM phosphate buffer (1:1 at pH 2) mobile phase. Gradient duration was 3–6 min depending on the sample (levofloxacin, and timolol). In the UPLC analysis, the LLOQs were 0.5 μM for levofloxacin and timolol (calibration curves are available in supplementary material).

2.5. Data analysis and simulations

2.5.1. Drug release from melanin and melanosomes

Sips isotherm was fitted to the experimental release data from melanin that assumes several binding modes of the drug on heterogenous melanin surfaces [28]. Fitting was based on the following equations:

$$\frac{d}{dt}(L) = -k_{on}.L^{n}.M + k_{off}.LM \quad (1)$$

$$\frac{d}{dt}(M) = -k_{on}.L^{n}.M + k_{off}.LM \quad (2)$$

$$\frac{d}{dt}(LM) = k_{on}.L^{n}.M - k_{off}.LM \quad (3)$$

where L, n, M, and LM correspond to the concentrations of free ligand (L), heterogeneity index (n), available (M) and occupied binding sites (LM). The equilibrium dissociation constant (K_d), and the rate constants for association (k_{on}) and dissociation (k_{off}) are presented as follows:

$$K_d^n = \frac{k_{off}}{k_{on}} \quad (4)$$

Other parameters, such as K_d (μM), n, and maximum binding capacity (B_{max}, nmol.mg^{-1}) are available from the literature (See Table 2) [21,29]. The total concentration of binding sites (M_{tot}) was calculated based on melanin concentration (M_0) and B_{max} as follows:

$$M_{tot} = M_0.B_{max} \quad (5)$$

The curve fitting was performed with Berkeley Madonna software (v 10.2.8, University of California, Berkeley, CA) using Rosenbrock (stiff) integration with the time step fixed at 0.0001 min to estimate k_{off} for each compound. The codes for the model are available in the supplementary information (Supplementary Table S2).

A similar curve fitting procedure was applied to the release data from melanosome experiments to estimate apparent dissociation rate constants (app k_{off}) from melanosomes. This parameter depends on k_{off} from melanin particles (within melanosomes) and the melanosomal membrane permeability of the drug.

2.5.2. Simulation of drug release from pigmented cells

The model for drug release from ARPE19-mel cells was built using Stella Professional version 2.1.4 (Isee systems, Lebanon, NH, USA). This bottom-up model (Fig. 1) was developed based on previous principles [20]. The model parameters are shown in Table 1, assuming that only free drug is able to permeate across melanosomal membrane and plasma

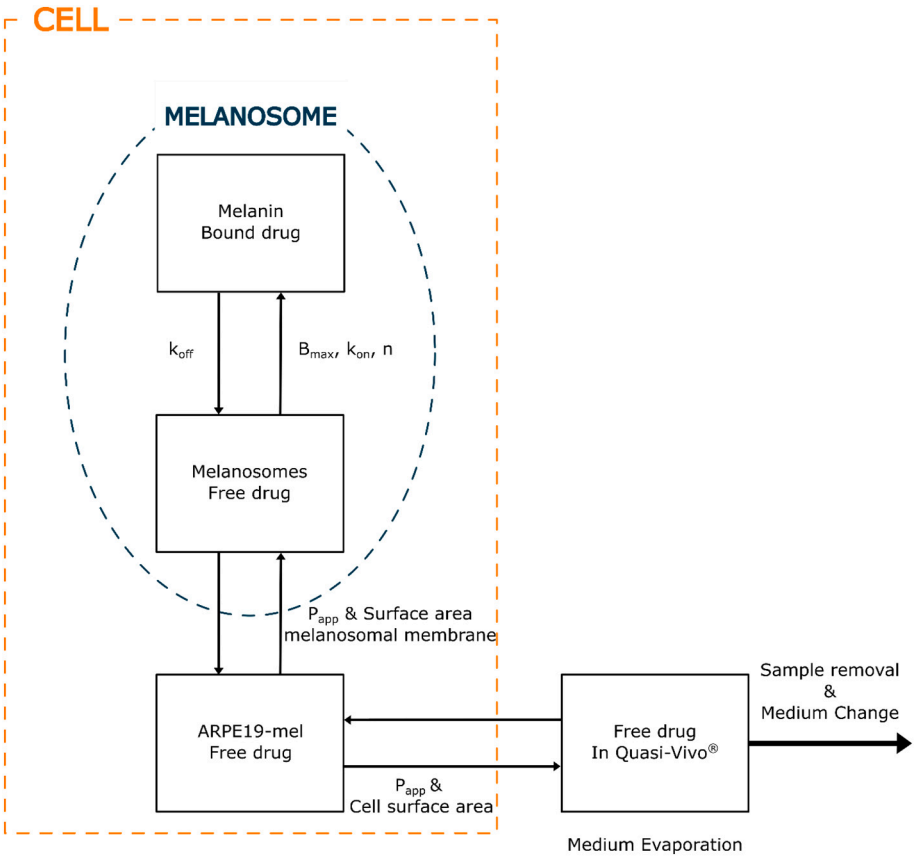

Fig. 1. Schematic structure of the model for drug release from melanosome-containing cells. All the drug in the cells is assumed to be melanin bound at time = 0. Dissociation and association rates to melanin are controlled by k_{off} and k_{on}. Identical apparent permeability (P_{app}) values were used for melanosomal and plasma membranes.

Table 1
Parameters used in the model and their values.

Parameters in model	Values	Reference/info
P_{app} in membrane (levofloxacin)	2.16×10^{-6} cm.s^{-1}	Calculated from Caco-2 cells [30]
	18×10^{-6} cm.s^{-1}	Calculated from LLC-PK1 cells [19]
P_{app} melanosomal membrane (levofloxacin)	$2–5 \times 10^{-6}$ cm.s^{-1}	Estimated from melanosomal drug release
P_{app} in membrane (timolol)	16.8×10^{-6} cm.s^{-1}	Calculated from isolated RPE-choroid of bovine eyes [33]
Amount of cellular melanin	138.5 μg ($n = 8$)	Experimental
Amount melanin (isolated melanosomes)	60 μg ($n = 20$)	Experimental
Amount of melanin (melanin study)	10 μg ($n = 12$)	Experimental
Medium volume	20 mL	Experimental
Evaporation rate	258 μL day^{-1}	Experimental
Inserted volume	350 μL day^{-1}	Experimental
Medium renewal (50%)	Day 4 and 7	Experimental
Cell number	165,000 cells/coverslip ($n = 7$)	Experimental
Coverslip surface area	1.13 cm^2	Experimental
Volume of ARPE19-mel cells	1.65 μL	Calculated from [34]
Melanosomal volume fraction	0.07	[35]
Surface area of melanosomes in the cell experiment	1.39 cm^2	Calculated assuming spherical shape with a diameter of 1 μm

membrane. Epithelial permeability studies report apparent permeabilities in cell monolayers (incl. Apical and basolateral membranes). Permeability values for single membranes were estimated as follows:

$$\frac{1}{P_{app,total}} = \frac{1}{P_{app,apical}} + \frac{1}{P_{app,basolateral}} \quad (6)$$

Thus,

$$P_{app,apical\ or\ basolateral} = 2 \times P_{app,total} \quad (7)$$

where, $P_{app,\ total}$ is the apparent permeability of a cell monolayer and $P_{app,\ apical\ or\ basolateral}$ denotes permeability in a single membrane (apical or basolateral). The medium volume was 20 mL; evaporation rate and added compensatory volumes were taken into account in the model. Thus, the rate of transport from inside the melanosomes to the cell cytosol can be written as:

$$Net\ rate\ of\ transport = P_{app,appical\ or\ basolateral} \times SA \times \left(C_{Mel} - C_{Cytosol}\right) \quad (8)$$

where permeation rate is controlled by the surface area (SA) of melanosomes and the unbound concentration difference between melanosomes (C_{mel}) and cytosol ($C_{cytosol}$). The same principles can be written for drug flux across cellular plasma membrane to the extracellular space. We assume similar permeability for melanosomal and plasma membrane, and a coverslips SA of 1.13 cm^2 for the cell compartment. The confluent coverslips contained 165,000 ± 6500 cells and their melanin contents were determined at the end of the release study. Knowing the fraction of melanosomes (0.07) in 100% pigmentation control cells (250 μg per 60,000 cells) [24], we estimated melanosomal SA in the experiment (Table 1). There were ~ 20% non-specific binding to plastic components of Quasi Vivo® for timolol. This factor was taken into account in the simulation model.

The interplay of parameters in the model was evaluated as follows: a) a 2–5 fold range of calculated k_{off}; values were used; b) melanin content from the experiment and higher amounts (range of 20–100% pigmentation per SA) were simulated; c) melanosomal SA was simulated over 25-fold range (0.3–5 cm^2); d) compound's specific permeability from the literature (Table 1) [10,19,30,31]. Finally, in order to further explore the interplay between melanosomal membrane properties and compound release, a relevant melanosomal SA to melanin content was selected for three cases with binding parameters (incl. k_{off}) of timolol, levofloxacin, and terazosin. Next, a wide range of hypothetical permeabilities ($0.1–100 \times 10^{-6}$ cm.s^{-1}) was tested using their respective binding parameters from Table 2.

In order to depict the impact of melanin content, we performed another simulation using a biologically relevant dose of 9.4 μg levofloxacin per coverslips. Since binding at equilibrium will require long incubation time, we only considered 90% of bound drug (relative to equilibrium point) for release simulation from different pigmentation levels. This is equivalent to the intravitreal injection of 0.1 mg levofloxacin to the human eye (retinal surface area: 12.04 cm^2 [32]).

3. Results

3.1. Drug release from melanin particles

Based on previous *in vitro* melanin binding studies [21,29], compounds with different melanin binding properties (timolol, levofloxacin, papaverine, terazosin) were selected (Table 2). Drug release data (Table 3) and profiles (Fig. 2) showed remarkable differences among the compounds, release times ranging from less than one hour (timolol) to a few hours (other compounds). The dissociation rate constants for high to extreme melanin binders (levofloxacin, papaverine, and terazosin) were 0.46–0.47 h^{-1}, while intermediate binder timolol showed k_{off} of 7.23

Table 2
Sips isotherm binding parameters for drug binding to melanin (mean ± SE) at pH 7.4.

Compound[a]	K_d ± SE (μM)	B_{max} ± SE (nmol.mg^{-1})	n ± SE	k[b] ± SE	Binding class
Timolol	120 ± 30	39 ± 6	0.95 ± 0.03	0.42 ± 0.02	intermediate
Levofloxacin	157 ± 56	72 ± 23	0.73 ± 0.02	1.82 ± 0.58	intermediate-high
Papaverine	66 ± 18	66 ± 6	0.72 ± 0.02	3.29 ± 0.76	high
Terazosin	46 ± 16	112 ± 13	0.64 ± 0.02	9.52 ± 2.45	high-extreme

[a] Binding parameters were collected from previous studies [21,29]. [b] $k \equiv B_{max}/K_d^n$.

Table 3
Dissociation rate constants of the drugs from melanin (k_{off}) and apparent dissociation rate constants from melanosomes (apparent k_{off}).

Compounds	$k_{off}(h^{-1})$ (melanin)	apparent $k_{off}(h^{-1})$ (melanosomes)
Timolol	7.23	0.97
Levofloxacin	0.47	0.32
Papaverine	0.46	0.36
Terazosin	0.46	0.20

h^{-1} (Table 3). K_d and B_{max} values showed clear differences among the compounds and the mean heterogeneity index (n) of Sips isotherm were 0.64–0.95 (Table 2).

3.2. Drug release from melanosome

The apparent k_{off} values describing the drug release from melanosomes were smaller than the corresponding k_{off} values from pure melanin (Table 3). For instance, dissociation of timolol from the melanosomes was ≈ 8 times slower than from melanin, while the differences between melanin and melanosomes were ≈ 1.3–2.3 fold for the other compounds. Then, we simulated drug release from melanin (with identical melanin content in the melanosomes) using experimental k_{off} values and compared these simulations with experimental and simulated drug release from the melanosomes (Fig. 3). Obviously, the melanosomal membrane slows down release, particularly in the case of timolol and terazosin (Fig. 3).

Thereafter, we simulated drug release from melanosomes by utilizing similar surface area and melanin content but using unique binding parameters for each drug (Tables 2-3). Theoretical permeability values were screened for melanosomal membranes to illustrate the impact of the membrane permeability on drug release (Fig. 4). Changes in membrane permeability have a remarkable impact on release and such effects were evident at realistic values of permeability coefficients (10^{-7}–10^{-5} $cm.s^{-1}$). The simulations suggest that the drug amount associated in melanosomes at 24 h was in the range of 0.5–3% in most cases, whereas this estimate for terazosin was below 10%.

3.3. Drug release from pigmented cells

Levofloxacin and timolol, two drugs with different dissociation rates and melanin binding, were selected for the cell studies. The cumulative release was followed until the plateau. Timolol showed non-specific binding in the range of 20% to Quasi Vivo® component during the six-day assay, but levofloxacin expressed no binding to the system. Timolol was released from the cells within 24 h, whereas levofloxacin showed retention for 11–13 days (Fig. 5).

Levofloxacin simulations showed that cell permeability has a significant effect on drug release from the cells, whereas 2-fold difference in k_{off} did not affect cellular drug retention and 5-fold change resulted in slight impact on the release rate (Fig. 5). Permeability change (2.2×10^{-6} $cm.s^{-1}$; 18×10^{-6} $cm.s^{-1}$) for levofloxacin resulted in 7-fold difference in the release rate at which 90% release was obtained (Fig. 6). On the other hand, five-fold variation in melanosomal surface area did not affect the final release rate, whereas assuming 10 times higher surface area caused 20–30% reduction in the final release rate (data not shown).

Levofloxacin release from pigmented cells, melanosomes, and

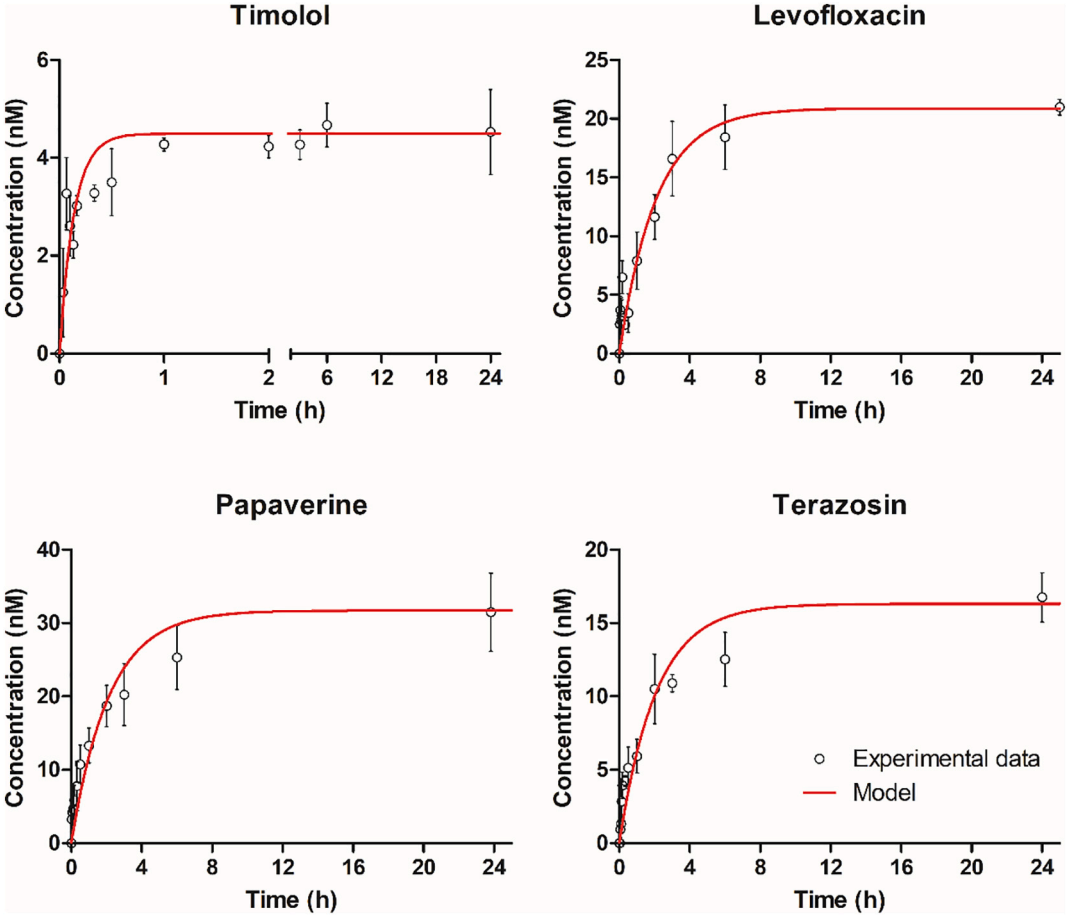

Fig. 2. Drug release from melanin *in vitro*. Experimental data points (open dots) and fitted dissociation curves (solid lines) are shown for timolol, levofloxacin, papaverine, and terazosin. Y-axis represents free compound concentration and error bars describe the standard deviations (n = 3–6).

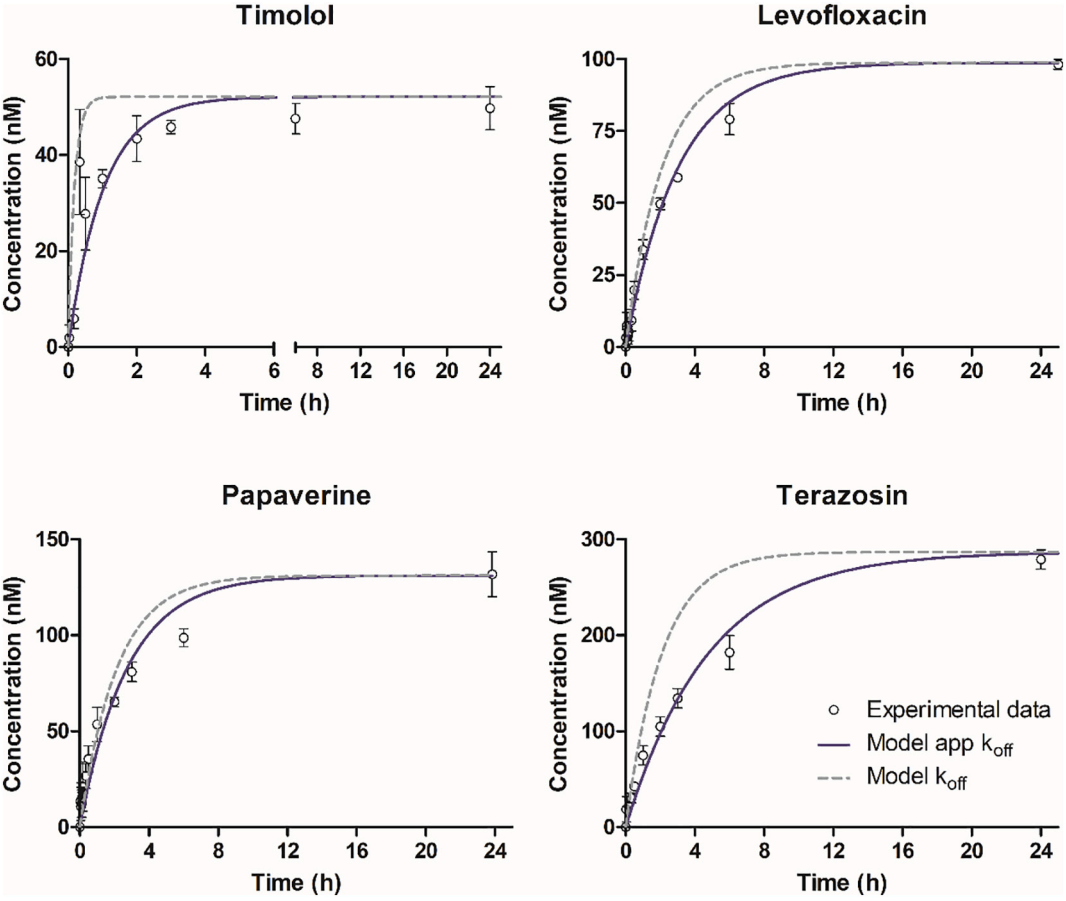

Fig. 3. Drug release from melanosomes. Open dots represent experimental data and solid lines are fitted data with an apparent dissociation rate constant (app k_{off}) using the kinetic simulation model. A hypothetical drug release from melanin (dashed lines) was simulated using experimental k_{off} from melanin release studies. The error bars represent the standard deviation (n = 3–6).

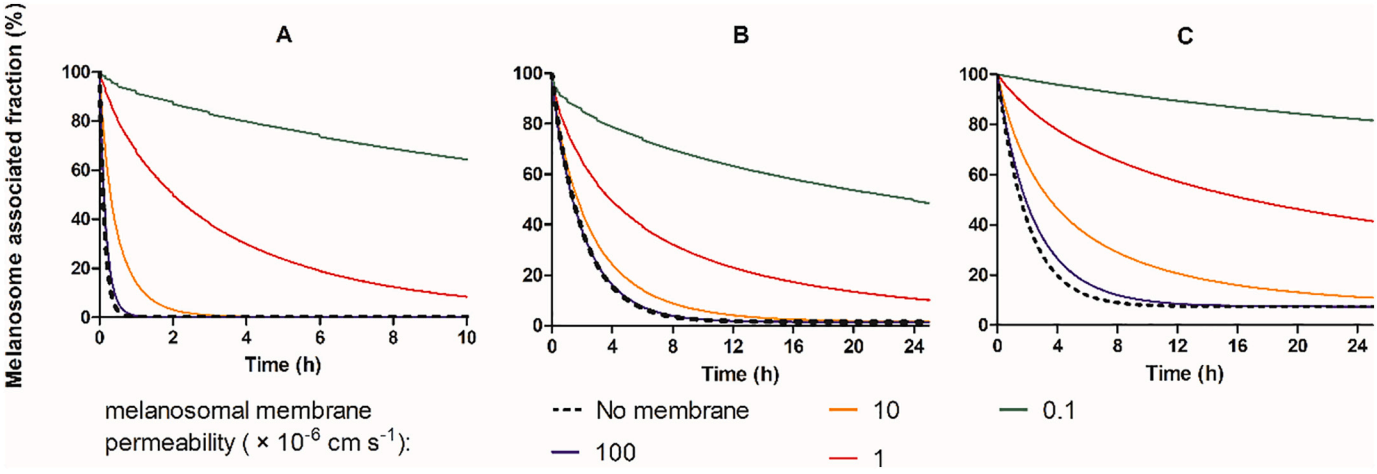

Fig. 4. Simulated release of timolol (A), levofloxacin (B), and terazosin-like (C) drugs from melanosomes at different melanosomal membrane permeabilities (solid lines, × 10^{-6} cm.s^{-1}). The dashed lines are simulated drug release profiles from melanin particles (no membrane). In all cases, similar melanin content and melanosomal surace area (Table 1) were used. In some cases, dashed lines are overlapped by solid lines indicating that the melanosome membrane does not limit drug release.

melanin were simulated with identical melanin content and melanin affinity (Fig. 6). Drug release of 90% from melanin, melanosome, and pigmented cells took place in 5, 20, and 120 h, respectively (Fig. 6). The intermediate binder timolol showed the faster release as all drug was released in <24 h.

The simulations on levofloxacin release from the cells at three different pigmentation levels (100% representing the levels in the human RPE) revealed that melanin content has remarkable effect on drug retention in the pigmented cells (Fig. 7). First, identical initial quantity of melanin bound levofloxacin was simulated at three levels of

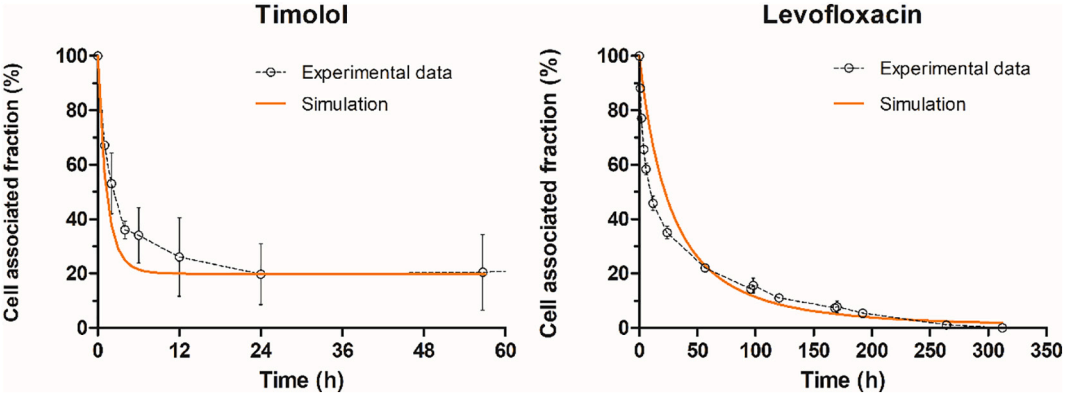

Fig. 5. Dissociation of timolol (left) and levofloxacin (right) from ARPE19-mel cells (open dots) and simulation (solid lines). Nonspecific binding of timolol to QuasiVivo components was taken into account in the simulations. Standard deviations are reported as error bars ($n = 3$).

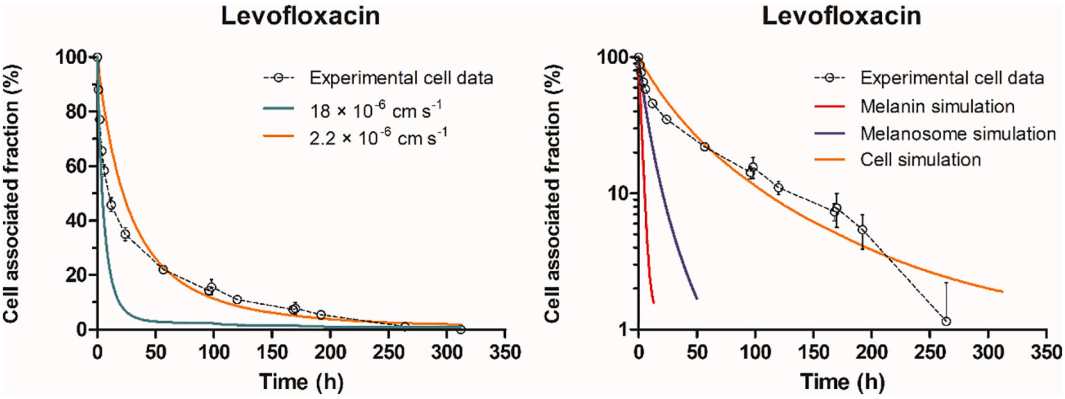

Fig. 6. LEFT. Simulation of levofloxacin release from the pigmented cells using two different membrane permeability values. The circles represent the mean ± S.D. of the experimental results. RIGHT. Drug release curves from melanin, melanosomes and cells were predicted using the permeability of 2.2×10^{-6} cm.s^{-1} in the membranes. Open circles and error bars represent mean experimental data ± S.D. (n = 3) from ARPE19-mel experiments.

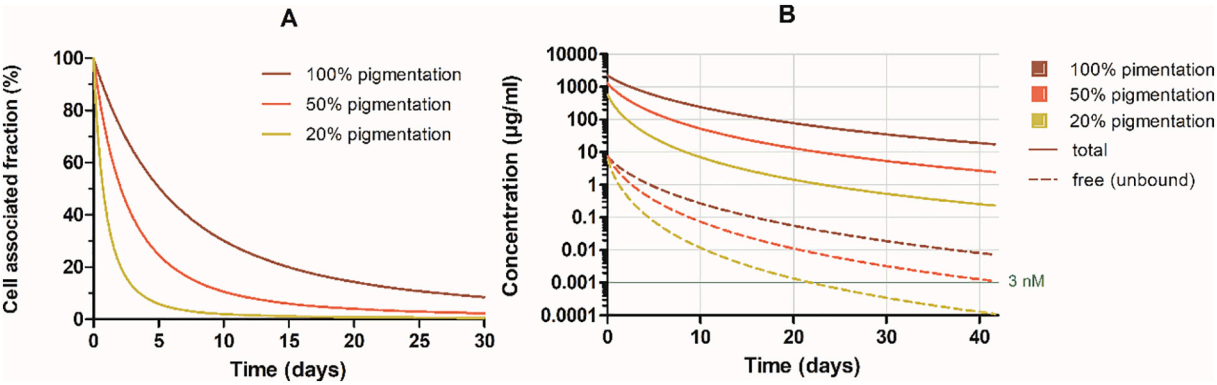

Fig. 7. A) Simulation of levofloxacin's release at three different pigmentation levels comparable to human RPE with identical drug associated with melanin. B) Levofloxacin simulation after incubating 9.4 µg drug to pigmented cells, using 90% of equilibrium bound amount as initial bound concentration at $t = 0$. Solid lines represent the total drug concentration associated with the cells, and dashed lines represent the free levofloxacin concentrations in the cell cytosol.

pigmentation. Time to release 90% of the drug increased from 3 to 27 days at 20% and 100% pigmentation, respectively. Secondly, higher levels of melanin resulted in nearly two orders of magnitude increase in total and free drug concentrations at 20–100% melanin contents when incubation with fixed 9.4 µg of levofloxacin was simulated. If minimum active concentration of levofloxacin would be 0.001 µg.mL^{-1} (≈3 nM) (Fig. 7B), the durations of drug action range from ≈ 20–80 days at pigmentation levels of 20–100%. However, at minimum inhibitory concentrations of 2 µg/mL only short duration of action is expected. The simulations with timolol and levofloxacin-like compound suggests that melanin can reduce the unbound melanosomal concentrations by 4–5 log for levofloxacin-like high binder, and 3 log units for intermediate binder (Fig. 8). In all cases, the ratio between unbound and bound fractions remained essentially constant over time. Thus, at any given time point, only very small fraction of melanosomal drug is available for permeation to the cytosol and further to the extracellular space.

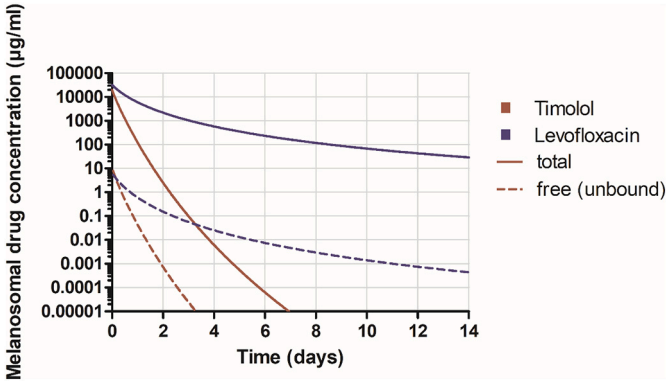

Fig. 8. Simulation of total and free levofloxacin and timolol-like compounds in the RPE cell melanosomes. Pigmentation levels comparable to human RPE were used in the simulation. Similar doses of levofloxacin and timolol (9.4 µg) were simulated using 90% levels of bound drug as the starting point (t = 0). Solid lines represent the total drug concentration associated with melanosomes, and dashed lines are the free concentration in the melanosomes. Identical membrane permeability was considered for both drugs in this simulation.

4. Discussion

Prior research has shown extensive drug retention and prolonged action in ocular pigmented tissues [14,15,36]. Melanin binding is a potential approach for targeted delivery to the pigmented tissues, such as the iris, ciliary body, RPE, and choroid. Nevertheless, drug retention in these tissues cannot be simply explained by the binding affinity of the drugs to melanin. For example, pilocarpine does not have significant binding *in vitro* [37–39], but it is retained 3–10 times more in the pigmented rabbit ocular tissues than in the corresponding albino rabbit tissues [40,41]. Moreover, papaverine has high affinity to melanin, but *in vivo* data shows elimination from the eye more rapidly than expected [19]. Dissociation of drugs from pure melanin is quick [19,42], but retention in the pigmented tissues can be substantially prolonged [19]. Rimpelä et al. developed a theoretical simulation model for drug dissociation from pigmented cells, but the experimental validation of the model was missing [20]. For this reason, we generated a drug release data and models for drug release from melanin, melanosomes, and pigmented cells. This was done to improve understanding of melanin binding in ocular pharmacokinetics.

Melanin. We explored drug dissociation from melanin particles by using high medium volume to ensure undisturbed drug dissociation. In addition, curve fitting was performed with Sips isotherm that considers the heterogeneous surface and multiple binding sites on the melanin particles [43]. The calculated k_{off} rates were similar for the high binders (papaverin, terazosin, and levofloxacin), translating to half-lives of about 1.5 h, which is significantly longer than the observed release half-life of timolol (≈ 6 min). As such, fast dissociation of drugs from melanin does not explain the ocular pharmacokinetics of melanin binding compounds.

Melanosomes. Dissociation of drugs from isolated melanosomes has been reported before [42,44], but there were major concerns regarding the purity of the isolated product. It is unclear whether the dissociation was studied with melanosomes, melanin, or their mixtures, because the preparations were not well-characterized. Herein, we used our recently published method [22] to produce a pure fraction of intact functional melanosomes. Our uptake and release study indicated higher drug loading in melanosomes than in melanin. This is related to the higher melanin content in the melanosome samples. Our dissociation model for drug release from melanosomes and melanin indicated that the melanosomal membrane slowed drug dissociation of all four compounds as evidenced by the apparent k_{off} values that were smaller than k_{off} values for identical melanin amounts (Table 3, Fig. 4). Furthermore, the release is affected by the free fraction of the drug within melanosomes, governed by the melanin affinity (Fig. 8). Taking into account these factors, it should be possible to tune drug release from melanosomes.

Pigmented cells. Drug release from pigmented cells has been studied *in vitro* [21], but it is difficult to maintain sink-conditions and avoid equilibration in small culture wells of conventional static cell cultures, particularly in the case of high melanin binders. Moreover, the melanosomes used for melanization must be intact, that was not the case in the release studies from re-pigmented bovine amelanotic RPE cells by Basu et al. [45]. We used a dynamic flow system (QuasiVivo®) to study the release of timolol and levofloxacin from pigmented ARPE19-mel cells. This approach enables the maintenance of sink conditions (high medium / cell ratio) and long-term cell viability (peristaltic flow and gas exchange) [46]. The peristaltic flow improves fluid dynamics as compared to static systems [47,48]. In this study, we used the pharmacologically relevant cell model, re-pigmented ARPE-19 cells [24], that express similar drug transporter profile to the primary human RPE cells [49]. Thus, we could grow cells containing intact melanosomes with a controlled degree of pigmentation to explore long-term retention of the drugs in these pigmented ARPE-19 cells. Although QuasiVivo® is a promising tool for long kinetic cell assays, non-specific binding to its large plastic surface area can be a challenge [26], as we observed for papaverine (data not shown). Also timolol bound to the plastic components of Quasi Vivo® (≈20%), but it was taken into account in the calculations and simulations. Overall, this experimental setup generates valuable parameters for simulation models that can be used to refine animal experiments.

The pigmented cells showed remarkably longer drug retention (1–2 weeks) than melanosomes (20h) or melanin (5 h). Based on our experimental data, we built simulation models to explore the interplay of different factors that contribute to the long drug retention in the pigmented cells (Table 1, Fig. 1). Importantly, the simulation of cellular drug release matched the experimental cell data from the dynamic flow system (Fig. 5). It is evident that the compound permeability across melanosomal and plasma membranes has a pronounced effect on the prolongation of drug retention in the pigmented cells. The simulations also showed that melanin binding can reduce the free concentration inside melanosomes to 3–5 order of magnitude for simulated compounds. Overall, it seems that the negligible free drug fraction in the melanosomes and the permeability in both melanosomal and cellular membranes contribute to the prolonged retention in pigmented cells compared to the short retention in the melanin particles.

There are inter-species differences in melanin content of the RPE [53] and unequal melanin distribution in the RPE [54,57]. Further, melanin content in the RPE decreases with aging (from 95 $\mu g.mg^{-1}$ at age of 14–50 to 22 $\mu g.mg^{-1}$ at ages >70 years) or due to certain ocular diseases [35,54,57]. Nonetheless, impact of aging on choroidal melanin remained to be determined [55,56]. On the other hand, the melanin concentration of RPE in the macular region remains steady and high suggesting that melanin targeting for posterior segment drug delivery is a relevant approach [54,55]. We measured melanin contents in the cells, which is important in the model validation. Further simulations with different melanin levels indicate that it has a major impact on drug release rate for two reasons. Firstly, higher levels of melanin in these cells are associated with higher uptake of the drug to pigmented cells. Secondly, a larger melanin content causes prolonging drug retention in pigmented cells, assuming that the same amount of drug is bound to melanin. In a study by Menon et al. bovine iris released 29% of bound timolol during 90 min, whereas the ciliary body with less melanin lost 52% of timolol in the same time [58]. Furthermore, they studied timolol release for the iris-ciliary body from albino, brown, gray, and black rabbits with different levels of melanin. Black rabbit iris-ciliary body took up more drug than the iris-ciliary body of brown rabbits, and retention was modestly longer in the tissue of black rabbits. Unfortunately, total melanin content per tissue was not reported in that study, but the different melanin content can potentially explain such

observations. Overall, our simulation model will be useful in predicting drug retention and concentrations in different species and situations with varying levels of melanin.

We used re-pigmented ARPE-19 cells that contain porcine melanosomes. Even though melanin is from pigs, the findings should be translatable to pigmented human tissues. Structure of melanin is similar in various species [9,20] and, consequently, binding of drugs to melanins of different origins is clearly translatable, even though the exact numbers of binding may vary [59]. Therefore, our conclusions should be clinically relevant.

Simulations. The simulation model was generated with the following assumptions: 1) All the bound drug is associated with melanin and not to the other cellular compartments. Other studies show that >90% of the drug can be associated within the melanosomes inside the pigmented RPE cells [24,34]; 2) The pigmentation level in the *in vitro* release study was ≈20% of the levels in the human RPE; 3) Cytosol is not a significant delaying barrier and the compounds are rapidly distributed within the cytosol [50–52]. Our model suggests that it is important to evaluate melanin content per surface of pigmented tissue for pre-clinical drug development phases, and special consideration should be given to interspecies translation. It should be noted that the confluent coverslips contained 146,000 cells.cm^{-2} (≈690 μg melanin), which is about half of the levels in the human RPE (295,000 cells.cm^{-2}) [32,60]. This suggests that there is about two times more melanin per surface area in the human RPE than in our experimental setting. The large melanin amounts may lead to the very long drug retention periods of weeks and months *in vivo*. Moreover, inter-species differences in ocular pharmacokinetics should be taken into account in drug discovery. For example, monkey eyes have 10–20 times more melanin in RPE-choroid than human RPE [53,61]. Higher melanin content may lead to greater drug accumulation, potentially overestimating clinical drug retention. Furthermore, varying melanin contents in different ocular tissues have pharmacological implications [61]. In particular, human choroid has substantially higher melanin content than the RPE [54,56], suggesting significant melanin bound drug depot in the choroid after ocular and systemic administration [11,62,63].

Free drug concentration in the pigmented cells or in their vicinity is critical from the viewpoint of pharmacological responses. Melanin binding is governed by the compound's affinity to melanin, but free drug concentrations in the cytosol and extracellular tissue space are affected also by the free drug concentration in the melanosomes and membrane permeability of the compound. Therefore, low-affinity melanin binder might lead to higher free cellular drug concentrations than a high binder drug, even though the retention would be shorter [21,27]. Jakubiak et al. demonstrated a strong correlation between drug accumulation to the pigment *in vitro* and *in vivo*, but drug retention in the pigmented tissues did not show as great correlation with melanin binding *in vitro* [19]. Such observations highlight the importance of the interplay between melanin binding and permeability factors, as membrane permeability also affects cellular retention of drugs in the pigmented cells. Access of drug to the melanosomes is also dependent on the membrane permeability and adequate permeability is a prerequisite of drug binding to melanin *in vivo*. Overall, a permeability should be be taken into account in discovery of melanin binding drugs.

In summary, membrane permeability, affinity to melanin and melanin content are critical determinants of final drug levels and retention in the pigmented eye tissues, such as the RPE and choroid. High affinity to melanin increases drug loading to melanosomes and keeps the free melanosomal concentration at low levels, thereby prolonging drug release from the melanosomes. Membrane permeability determines access of drug to melanosomes well as the rate for free drug permeation from the melanosomes to cytosol and extracellular space. The interplay of permeability and melanin binding is useful information in ocular drug discovery and development as these factors could be taken into account when routes of drug administration, doses and dosing frequencies and drug delivery systems are designed.

5. Conclusion

Drug retention in pigmented tissues is controlled by the drug permeability in the cell membranes, binding to melanin, unbound fraction of drug in the melanosomes and melanin content in the cells. Drug release rate is remarkably slower from the pigmented cells as compared to isolated melanin and melanosomes. The dynamic flow system enabled us to study drug retention in pigmented tissues for a long periods. The mechanistic simulation model showed acceptable match with the experimental data and provides a tool for sensitivity analyses and predictions in drug development.

Conflict of interest

None.

Acknowledgements

Arto Urtti is grateful to Academy of Finland (grant 343138) and Government of Russian Federation (Mega Grant, agreement 075-15-2021-637). Sina Bahrpeyma acknowledges Doctoral School of the University of Eastern Finland, Instrumentarium Science Foundation, Eye and Tissue Bank Foundation (Silmä- ja kudospankkisäätiö), and Sokeain Ystävät. Dr. Laura Hellinen acknowledges funding from Academy of Finland (grant 333903). Eva M. del Amo was supported by the strategic funding of the University of Eastern Finland. We thank Dr. Tatu Lajunen, Eija Mäki-Mikola, and Senni Anturaniemi for their help in technical aspects of dynamic flow system. The UPLC analysis was kindly done by Timo Oksanen. Riikka-Juulia Lepistö is thanked for the technical assistance with LC-MS/MS instrument. We acknowledge Biocenter Finland Infrastructure Drug Discovery and Chemical Biology for enabling the LC/MS analytics at the University of Helsinki. The eyeball Anatomy in the graphical abstract was created using BioRender (https://biorender.com/).

Appendix A. Supplementary data

Supplementary data to this article can be found online at https://doi.org/10.1016/j.jconrel.2022.05.059.

References

[1] A. Urtti, Challenges and obstacles of ocular pharmacokinetics and drug delivery, Adv. Drug Deliv. Rev. 58 (2006) 1131–1135.
[2] C.O. Okeke, H.A. Quigley, H.D. Jampel, G. Ying, R.J. Plyler, Y. Jiang, D. S. Friedman, Interventions improve poor adherence with once daily glaucoma medications in electronically monitored patients, Ophthalmology. 116 (2009) 2286–2293.
[3] O. Rahić, A. Tucak, N. Omerović, M. Sirbubalo, L. Hindija, J. Hadžiabdić, E. Vranić, Novel drug delivery systems fighting glaucoma: formulation obstacles and solutions, Pharmaceutics. 13 (2021) 28.
[4] C. Jumelle, S. Gholizadeh, N. Annabi, R. Dana, Advances and limitations of drug delivery systems formulated as eye drops, J. Control. Release 321 (2020) 1–22.
[5] E.M. Del Amo, A.-K. Rimpelä, E. Heikkinen, O.K. Kari, E. Ramsay, T. Lajunen, M. Schmitt, L. Pelkonen, M. Bhattacharya, D. Richardson, Pharmacokinetic aspects of retinal drug delivery, Prog. Retin. Eye Res. 57 (2017) 134–185.
[6] D.M. Maurice, S. Mishima, M. Sears, Pharmacology of the eye, Handb. Exp. Pharmacol. 69 (1984) 19–116.
[7] E.M. del Amo, K.-S. Vellonen, H. Kidron, A. Urtti, Intravitreal clearance and volume of distribution of compounds in rabbits: in silico prediction and pharmacokinetic simulations for drug development, Eur. J. Pharm. Biopharm. 95 (2015) 215–226.
[8] E.M. Del Amo, A. Urtti, Current and future ophthalmic drug delivery systems: a shift to the posterior segment, Drug Discov. Today 13 (2008) 135–143.
[9] D. Hu, J.D. Simon, T. Sarna, Role of ocular melanin in ophthalmic physiology and pathology, Photochem. Photobiol. 84 (2008) 639–644.
[10] L. Pitkänen, V.P. Ranta, H. Moilanen, A. Urtti, Binding of betaxolol, metoprolol and oligonucleotides to synthetic and bovine ocular melanin, and prediction of drug binding to melanin in human choroid-retinal pigment epithelium, Pharm. Res. 24 (2007) 2063–2070, https://doi.org/10.1007/s11095-007-9342-0.
[11] M. Tanaka, C. Ono, M. Yamada, Absorption, distribution and excretion of 14C-levofloxacin after single oral administration in albino and pigmented rats: binding characteristics of levofloxacin-related radioactivity to melanin in vivo, J. Pharm. Pharmacol. 56 (2004) 463–469.

[12] M. Araie, M. Takase, Y. Sakai, Y. Ishii, Y. Yokoyama, M. Kitagawa, Beta-adrenergic blockers: ocular penetration and binding to the uveal pigment, Jpn. J. Ophthalmol. 26 (1982) 248–263.

[13] K. Shinno, K. Kurokawa, S. Kozai, A. Kawamura, K. Inada, H. Tokushige, The relationship of brimonidine concentration in vitreous body to the free concentration in retina/choroid following topical administration in pigmented rabbits, Curr. Eye Res. 42 (2017) 748–753.

[14] M. Salazar, P.N. Patil, An explanation for the long duration of mydriatic effect of atropine in eye, Invest. Ophthalmol. Vis. Sci. 15 (1976) 671–673.

[15] A. Urtti, L. Salminen, H. Kujari, V. Jäntti, Effect of ocular pigmentation on pilocarpine pharmacology in the rabbit eye. II. Drug response, Int. J. Pharm. 19 (1984) 53–61.

[16] S.J. Robbie, P.L. von Leithner, M. Ju, C.A. Lange, A.G. King, P. Adamson, D. Lee, C. Sychterz, P. Coffey, Y.-S. Ng, Assessing a novel depot delivery strategy for noninvasive administration of VEGF/PDGF RTK inhibitors for ocular neovascular disease, Invest. Ophthalmol. Vis. Sci. 54 (2013) 1490–1500.

[17] P. Jakubiak, M. Reutlinger, P. Mattei, F. Schuler, A. Urtti, R. Alvarez-Sánchez, Understanding molecular drivers of melanin binding to support rational Design of Small Molecule Ophthalmic Drugs, J. Med. Chem. 61 (2018) 10106–10115, https://doi.org/10.1021/acs.jmedchem.8b01281.

[18] J. Reilly, S.L. Williams, C.J. Forster, V. Kansara, P. End, M.H. Serrano-Wu, High-throughput melanin-binding affinity and in silico methods to aid in the prediction of drug exposure in ocular tissue, J. Pharm. Sci. 104 (2015) 3997–4001.

[19] P. Jakubiak, C. Cantrill, A. Urtti, R. Alvarez-Sánchez, Establishment of an in vitro-in vivo correlation for melanin binding and the extension of the ocular half-life of small-molecule drugs, Mol. Pharm. (2019), https://doi.org/10.1021/acs.molpharmaceut.9b00769.

[20] A.K. Rimpelä, M. Reinisalo, L. Hellinen, E. Grazhdankin, H. Kidron, A. Urtti, E. M. del Amo, Implications of melanin binding in ocular drug delivery, Adv. Drug Deliv. Rev. 126 (2018) 23–43, https://doi.org/10.1016/j.addr.2017.12.008.

[21] A.K. Rimpelä, M. Schmitt, S. Latonen, M. Hagström, M. Antopolsky, J. A. Manzanares, H. Kidron, A. Urtti, Drug distribution to retinal pigment epithelium: studies on melanin binding, cellular kinetics, and single photon emission computed tomography/computed tomography imaging, Mol. Pharm. 13 (2016) 2977–2986, https://doi.org/10.1021/acs.molpharmaceut.5b00787.

[22] L. Pelkonen, M. Reinisalo, E. Morin-Picardat, H. Kidron, A. Urtti, Isolation of intact and functional melanosomes from the retinal pigment epithelium, PLoS One 11 (2016) 1–13, https://doi.org/10.1371/journal.pone.0160352.

[23] K.C. Dunn, A.E. Aotaki-Keen, F.R. Putkey, L.M. Hjelmeland, ARPE-19, a human retinal pigment epithelial cell line with differentiated properties, Exp. Eye Res. 62 (1996) 155–170.

[24] L. Hellinen, M. Hagström, H. Knuutila, M. Ruponen, A. Urtti, M. Reinisalo, Characterization of artificially re-pigmented ARPE-19 retinal pigment epithelial cell model, Sci. Rep. 9 (2019) 1–10, https://doi.org/10.1038/s41598-019-50324-8.

[25] D. Mazzei, M.A. Guzzardi, S. Giusti, A. Ahluwalia, A RTICLE A Low Shear Stress Modular Bioreactor for Connected Cell Culture Under High Flow Rates 106 (2010) 127–137, https://doi.org/10.1002/bit.22671.

[26] T. Sbrana, A. Ahluwalia, Engineering Quasi-Vivo® in Vitro Organ Models, in: M. Balls, R.D. Combes, N. Bhogal (Eds.), New Technol. Toxic. Test, Springer, US, New York, NY, 2012, pp. 138–153, https://doi.org/10.1007/978-1-4614-3055-1_9.

[27] A.K. Rimpelä, M. Hagström, H. Kidron, A. Urtti, Melanin targeting for intracellular drug delivery: quantification of bound and free drug in retinal pigment epithelial cells, J. Control. Release 283 (2018) 261–268, https://doi.org/10.1016/j.jconrel.2018.05.034.

[28] R. Sips, On the structure of a catalyst surface, J. Chem. Phys. 16 (1948) 490–495.

[29] L. Hellinen, S. Bahrpeyma, A. Rimpelä, M. Hagström, M. Reinisalo, A. Urtti, Microscale thermophoresis as a screening tool to predict melanin binding of, Drugs (2020) 1–13.

[30] D.A. Volpe, Permeability classification of representative fluoroquinolones by a cell culture method, AAPS PharmSci. 6 (2004) 1–6.

[31] S.M. Robertson, M.A. Curtis, B.A. Schlech, A. Rusinko, G.R. Owen, O. Dembinska, J. Liao, D.C. Dahlin, Ocular Pharmacokinetics of Moxifloxacin After Topical Treatment of Animals and Humans 50 (2005), https://doi.org/10.1016/j.survophthal.2005.07.001.

[32] S. Panda-Jonas, J.B. Jonas, M. Jakobczyk, U. Schneider, Retinal photoreceptor count, retinal surface area, and optic disc size in normal human eyes, Ophthalmology. 101 (1994) 519–523.

[33] L. Pitkänen, V.-P. Ranta, H. Moilanen, A. Urtti, Permeability of retinal pigment epithelium: effects of permeant molecular weight and lipophilicity, Invest. Ophthalmol. Vis. Sci. 46 (2005) 641–646.

[34] A.K. Rimpelä, M. Hagström, H. Kidron, A. Urtti, Melanin targeting for intracellular drug delivery: quantification of bound and free drug in retinal pigment epithelial cells, J. Control. Release 283 (2018) 261–268, https://doi.org/10.1016/j.jconrel.2018.05.034.

[35] L. Feeney-Burns, E.S. Hilderbrand, S. Eldridge, Aging human RPE: morphometric analysis of macular, equatorial, and peripheral cells, Invest. Ophthalmol. Vis. Sci. 25 (1984) 195–200.

[36] M. Salazar, K. Shimada, P.N. Patil, Iris pigmentation and atropine mydriasis, J. Pharmacol. Exp. Ther. 197 (1976) 79–88.

[37] L. Pelkonen, K. Sato, M. Reinisalo, H. Kidron, M. Tachikawa, M. Watanabe, Y. Uchida, A. Urtti, T. Terasaki, LC-MS/MS based quantitation of ABC and SLC transporter proteins in plasma membranes of cultured primary human retinal pigment epithelium cells and immortalized ARPE19 cell line, Mol. Pharm. 14 (2017) 605–613, https://doi.org/10.1021/acs.molpharmaceut.6b00782.

[38] L. Pelkonen, U. Tengvall-Unadike, M. Ruponen, H. Kidron, E.M. del Amo, M. Reinisalo, A. Urtti, Melanin binding study of clinical drugs with cassette dosing and rapid equilibrium dialysis inserts, Eur. J. Pharm. Sci. 109 (2017) 162–168, https://doi.org/10.1016/j.ejps.2017.07.027.

[39] A. Nagata, H.K. Mishima, Y. Kiuchi, A. Hirota, T. Kurokawa, S. Ishibashi, Binding of antiglaucomatous drugs to synthetic melanin and their hypotensive effects on pigmented and nonpigmented rabbit eyes, Jpn. J. Ophthalmol. 37 (1993) 32–38.

[40] L. Salminen, A. Urtti, L. Periviita, Effect of ocular pigmentation on pilocarpine pharmacology in the rabbit eye. I. Drag distribution and metabolism, Int. J. Pharm. 18 (1984) 17–24.

[41] V.H.L. Lee, J.R. Robinson, Disposition of pilocarpine in the pigmented rabbit eye, Int. J. Pharm. 11 (1982) 155–165.

[42] P. AULA, T. KAILA, R. HUUPPONEN, L. SALMINEN, Timolol binding to bovine ocular melanin in vitro, J. Ocul. Pharmacol. Ther. 4 (1988) 29–36.

[43] J.A. Manzanares, A.K. Rimpelä, A. Urtti, Interpretation of ocular melanin drug binding assays. Alternatives to the model of multiple classes of independent sites, Mol. Pharm. 13 (2016) 1251–1257, https://doi.org/10.1021/acs.molpharmaceut.5b00783.

[44] P. Auld, Prostaglandin Fz, Binding to Bovine Ocular and Synthetic Melanins (1989) 100–103.

[45] P.K. Basu, I.A. Menon, S.D. Persad, J.D. Wiltshire, Binding of chlorpromazine to cultured retinal pigment epithelial cells loaded with melanin, Lens Eye Toxic. Res. 6 (1989) 229–240.

[46] B. Vinci, C. Duret, S. Klieber, S. Gerbal-Chaloin, A. Sa-Cunha, S. Laporte, B. Suc, P. Maurel, A. Ahluwalia, M. Daujat-Chavanieu, Modular bioreactor for primary human hepatocyte culture: medium flow stimulates expression and activity of detoxification genes, Biotechnol. J. 6 (2011) 554–564.

[47] S. Giusti, T. Sbrana, M. La Marca, V. Di Patria, V. Martinucci, A. Tirella, C. Domenici, A. Ahluwalia, A novel dual-flow bioreactor simulates increased fluorescein permeability in epithelial tissue barriers, Biotechnol. J. 9 (2014) 1175–1184.

[48] K. Kulthong, L. Duivenvoorde, H. Sun, S. Confederat, J. Wu, B. Spenkelink, L. de Haan, V. Marin, M. van der Zande, H. Bouwmeester, Microfluidic chip for culturing intestinal epithelial cell layers: characterization and comparison of drug transport between dynamic and static models, Toxicol. Vitr. 65 (2020), 104815.

[49] L. Hellinen, K. Sato, M. Reinisalo, H. Kidron, K. Rilla, M. Tachikawa, Y. Uchida, T. Terasaki, A. Urtti, Quantitative protein expression in the human retinal pigment epithelium: comparison between apical and basolateral plasma membranes with emphasis on transporters, Invest. Ophthalmol. Vis. Sci. 60 (2019) 5022–5034.

[50] S. Bicknese, N. Periasamy, S.B. Shohet, A.S. Verkman, Cytoplasmic viscosity near the cell plasma membrane: measurement by evanescent field frequency-domain microfluorimetry, Biophys. J. 65 (1993) 1272–1282.

[51] A.S. Verkman, Solute and macromolecule diffusion in cellular aqueous compartments, Trends Biochem. Sci. 27 (2002) 27–33.

[52] K. Luby-Phelps, Cytoarchitecture and physical properties of cytoplasm: volume, viscosity, diffusion, intracellular surface area, Int. Rev. Cytol. 192 (1999) 189–221.

[53] C. Durairaj, J.E. Chastain, U.B. Kompella, Intraocular distribution of melanin in human, monkey, rabbit, minipig and dog eyes, Exp. Eye Res. 98 (2012) 23–27. doi: https://doi.org/10.1016/j.exer.2012.03.004.

[54] J.J. Weiter, F.C. Delori, G.L. Wing, K.A. Fitch, Retinal pigment epithelial lipofuscin and melanin and choroidal melanin in human eyes, Invest. Ophthalmol. Vis. Sci. 27 (1986) 145–152.

[55] C.A. May, Chronologic versus Biologic Aging of the Human Choroid 2013 (2013).

[56] S. Hayasaka, Aging changes in lipofuscin, lysosomes and melanin in the macular area of human retina and choroid, Jpn. J. Ophthalmol. 33 (1989) 36–42.

[57] S.Y. Schmidt, R.D. Peisch, Melanin concentration in normal human retinal pigment epithelium. Regional variation and age-related reduction, Invest. Ophthalmol. Vis. Sci. 27 (1986) 1063–1067.

[58] I.A. Menon, G.E. Trope, P.K. Basu, D.C. Wakeham, S.D. Persad, Binding of Timolol to Iris-ciliary body and melanin : an in vitro model for assessing the kinetics and efficacy of long-acting Antiglaucoma, Drugs 5 (1989).

[59] P. Jakubiak, F. Lack, J. Thun, A. Urtti, R. Alvarez-Sanchez, Influence of melanin characteristics on drug binding properties, Mol. Pharm. 16 (2019) 2549–2556.

[60] S. Panda-Jonas, J.B. Jonas, M. Jakobczyk-Zmija, Retinal pigment epithelial cell count, distribution, and correlations in normal human eyes, Am J. Ophthalmol. 121 (1996) 181–189.

[61] B.G. Short, Safety evaluation of ocular drug delivery formulations: techniques and practical considerations, Toxicol. Pathol. 36 (2008) 49–62.

[62] A.-K. Rimpelä, M. Garneau, K.S. Baum-Kroker, T. Schönberger, F. Runge, A. Sauer, Quantification of drugs in distinctly separated ocular substructures of albino and pigmented rats, Pharmaceutics. 12 (2020) 1174.

[63] K.-S. Vellonen, E.-M. Soini, E.M. Del Amo, A. Urtti, Prediction of ocular drug distribution from systemic blood circulation, Mol. Pharm. 13 (2016) 2906–2911.